

A UHF RFID Tag Embeddable in Small Metal Cavities

Andrea Michel, *Member, IEEE*, Vittorio Franchina, Paolo Nepa, *Member, IEEE*, and Alfredo Salvatore

Abstract— A compact in-metal UHF RFID tag for identification of metal components is described. The radiating element is printed on a $23 \times 23 \times 1$ mm³ copper-clad Alumina (Al₂O₃) substrate ($\epsilon_r=9$, $\tan\delta=0.0003$) and consists of two rectangular quarter-mode patch antennas properly arranged to make the tag performance as robust as possible even when the tag is embedded in small cavities carved out of metal objects. The entire structure has been optimized by taking into account the presence of a thin superstrate of commercial epoxy resin used to protect the tag. The effect of the cavity size on the tag performance is numerically analyzed. Measurements on a tag prototype are also described and discussed.

Index Terms— Tag antenna, RFID, UHF, in-metal tag, metal embedded tag, quarter-mode patch.

I. INTRODUCTION

Most of the commercial Ultra High Frequency (UHF) Radio Frequency Identification (RFID) tags are represented by dipole-like antennas designed on paper or flexible adhesive plastic sheets [1]. They show high performance when applied to paper or plastic objects, allowing for long read ranges (even more than 10m). However, their performance drops down when pasted on metal surfaces or bottles containing liquids.

In the framework of metal-attachable UHF RFID tags, several antenna solutions have been proposed in the scientific literature [2]- [17]. The most common antenna layout considered for UHF RFID on-metal tags are inverted-F antenna, planar inverted-F antennas (PIFA) and patch-like structures. In [2], a $32 \times 18 \times 3.2$ mm³ tag antenna consisting of two rectangular patches electrically connected to the ground plane is proposed. In this solution, a conductive layer is inserted into the antenna structure to increase the capacitive reactance of the antenna. Despite the small antenna size, the UHF RFID tag can be detected up to 1.5m with an Effective Isotropic Radiated Power (EIRP) of 4W. A similar configuration is presented in [3]. In order to adjust the input impedance of UHF RFID tag antennas consisting of two quarter-wave patch antennas, in [4] the feeding network and the radiator have been designed separately. Specifically, the feeding network consists in a small loop printed in correspondence of the center of the slot between the two patches, and its dimensions are optimized to adapt the input impedance. In [5], a $25 \times 40 \times 3$ mm³ folded patch antenna designed on a flexible polyethylene terephthalate (PET) substrate is proposed, which achieves a maximum read range of 10m with an EIRP of 4W when attached on a metal object. Other examples of small and flexible metal mountable UHF RFID tags are described in [6], where a 30×30 mm² serrated folded patch is wrapped around a 3-mm-thick foam substrate, and in [7], where a 14×28 mm² antenna has been designed on a 1.5-mm-thick high-dielectric polymer-ceramic composite substrate. Recently, passive 2-D and 3-D RFID tag layouts have been fabricated using additive manufacturing processes such as fused deposition modeling (FDM) of thermoplastic and microdispensing of silver paste [8]. Loop-type antennas have also been considered for on-metal UHF RFID applications [9], [10]. Finally, PIFAs [11] and dipolar patches [12] mountable on a metal object are arranged in a cross configuration to achieve orientation insensitivity.

In a large number of metal objects such as aircraft, vehicles and shipping containers, recessed volumes already exist and may be exploited for UHF RFID tag, thus protecting the transponder from impacts or damages. Consequently, on-metal tags are being used also for “in-metal” applications [13]-[17]. In [13], a bowtie dipole antenna printed on a 1.63-mm-thick Taconic TRF-45 dielectric substrate is located inside a $140 \times 80 \times 50$ mm³ cavity with an open top. A numerical analysis is shown demonstrating that the cavity depth is crucial for the dipole antenna optimization. Also, in [14] a proximity coupled cavity backed patch antenna is designed on a $107 \times 70 \times 3.18$ mm³ cavity, where a π -network is included for fine impedance tuning. A measured gain of 5.7dBi is obtained, giving a reading range up to 23m. Furthermore, in [16], [17] the metal cavity is part of the tag antenna, which consists in two PIFAs designed on a circular (diameter of 34mm) 5-mm-thick ceramic material.

In this paper, a low-profile in-metal tag is designed to be embedded in thin cavities carved out of small metal parts. In applications where an assembly line is foreseen like in the automotive or aerospace field, metal components are transported by means of conveyor belts to an assembly area where human operators or automated systems are designated to build the final product. Thus, the presence of a small embedded and irremovable UHF RFID tag is helpful to automatically identify and locate each single metal part. The proposed tag consists of two miniaturized quarter-mode patch antennas properly arranged to make the tag less sensitive to the presence of the cavity metal walls. The presence of a commercial epoxy resin is taken into account during the design process, and exploited to reduce the tag antenna physical size. In Section II, the antenna design is described together with simulated results. In Section III, experimental results are presented. Finally, conclusions are drawn in Section IV.

II. ANTENNA LAYOUT AND NUMERICAL ANALYSIS

The proposed tag antenna has been designed starting from a microstrip patch antenna. Preliminary results have been described in [18]. The design steps are schematically represented in Fig. 1. The rectangular patch (Fig. 1a) has been designed on a 1-mm-thick alumina (Al₂O₃) substrate ($\epsilon_r=9$, $\tan\delta=0.0003$) [19]. When the patch resonating edge is slightly lower than $\lambda_g/2$ (being λ_g the equivalent waveguide wavelength at 866.5 MHz), the patch antenna input impedance is ohmic-inductive. The position of the input port can thus be chosen to match with the ohmic-capacitive impedance of the UHF RFID chip. In this analysis, an EPC Global Class-1 Gen-2 Higgs 4 IC (package SOT323) chip manufactured by Alien Technology [23], has been considered. Specifically, the chip impedance at the ETSI UHF RFID central frequency (i.e. 866MHz) is

$Z_{in}=20.55-j191.25\Omega$ [7]. Then, meanders have been introduced in the resonating edges to further reduce the electrical size of the patch antenna (Fig. 1b). By inserting vias connected to the ground plane, a quarter-wavelength patch antenna can be obtained (Fig. 1c), splitting in a half the antenna size with marginal modifications of its input impedance. In this way, the edge close to the input port remains the only radiating aperture of the microstrip antenna. In this region, the electric field is quite strong, and it could be significantly affected by the presence of a metal wall when the tag is placed inside a cavity.

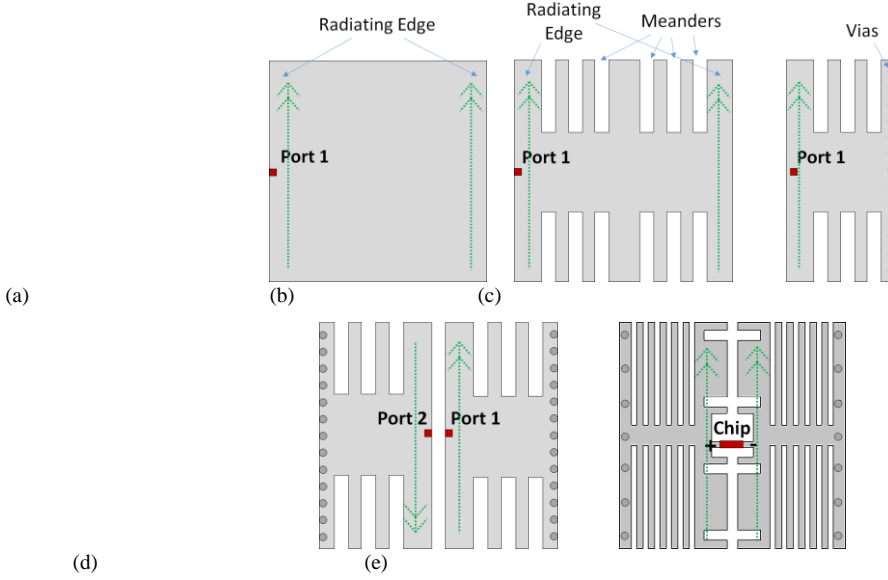


Fig. 1. Schematic representation of the design procedure followed to optimize the UHF RFID in-metal tag.

For this reason, a second quarter-wavelength patch antenna is arranged close to the open side of the first structure (Fig. 1d), with its port (Port 2) on the same side of Port 1. Hence, the two quarter-wavelength patch antennas radiate from the central slot between them, limiting the effect of the cavity walls. However, when the two antennas are fed with two in-phase currents, two out-of-phase electric field are radiated, resulting in a low radiation efficiency. For this reason, the two elements must be fed with out-of-phase currents. The final layout is shown in Fig. 1e, where the UHF RFID chip is attached to the edge of the two $25 \times 25 \times 1$ mm³ quarter-wavelength patches. The 3D layout of the antenna is shown in Fig. 2a. Initially, the antenna has been optimized on a $(L_M \times L_M)$ 500 \times 500 mm² metal plane ($1.45 \lambda_0 \times 1.45 \lambda_0$, being λ_0 the free space wavelength at 866.5 MHz), with a thickness H_M of 12mm. Thus, a $L_C \times L_C \times H_C$ cavity has been carved out of the metal object, and the effect of the cavity geometrical parameters has been numerically evaluated. The main parameters of the analyzed scenario are indicated in Fig. 2b.

In Fig. 3a, the antenna simulated performance is reported as a function of the square cavity edge, L_C , when the tag is completely embedded in the metal cavity ($H_C = 2$ mm). Numerical results have been obtained by means of the commercial software CST Microwave Studio[®]. The minimum value of L_C considered in this analysis is 27mm, which is only 2mm greater than the tag size. Indeed, from a practical point of view this minimum value guarantees an easy integration of the tag inside the cavity, so preventing the electrical contact between the tag metal parts and the cavity walls even though the tag is not perfectly aligned to the cavity center. The solid black line represents the frequency corresponding to the minimum of the Power Reflection Coefficient (PRC) [21]- [22], which is defined as

$$PRC = 1 - \tau = 1 - \frac{4R_{CHIP}R_{TAG}}{|Z_{CHIP} + Z_{TAG}|^2} \quad (1)$$

where $Z_{TAG} = R_{TAG} + jX_{TAG}$ and $Z_{CHIP} = R_{CHIP} + jX_{CHIP}$ represent the tag antenna input impedance and the Higgs 4 IC chip impedance [23], respectively. The PRC indicates the matching between the antenna input impedance and the chip impedance, and it can be used instead of the power transmission coefficient (τ) [20], by analogy with the reflection coefficient typically used by antenna designers. The transversal red bars indicate the frequency range in which the simulated PRC assumes values lower than -3dB, which are considered enough to guarantee a satisfactory read range [21], [22]. Finally, the blue dashed line represents the simulated gain along the z -axis as a function of the cavity size, which also corresponds to the maximum gain. It is worth noting that both the antenna resonance frequency and gain remain stable for different values of L_C , while the half-power bandwidth ($PRC < -3$ dB) is always wider than the ETSI UHF RFID band (865-868 MHz).

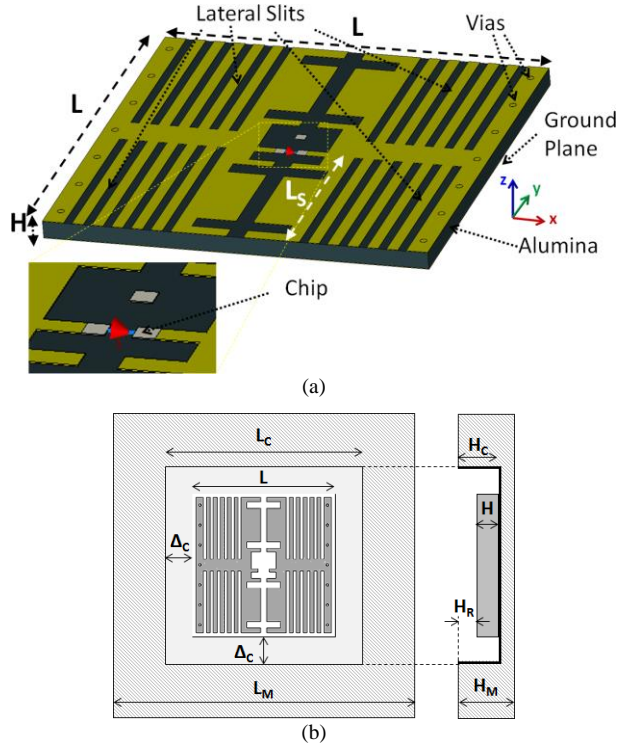


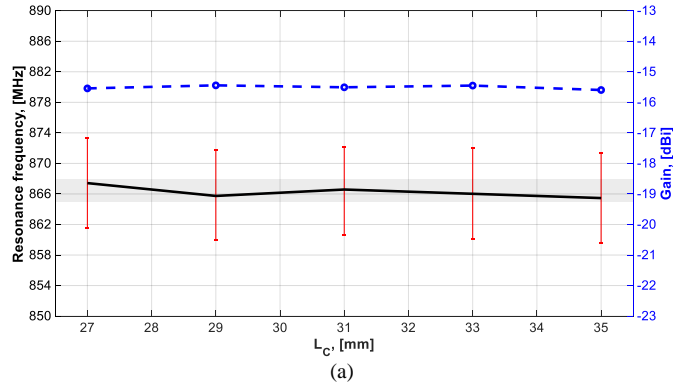
Fig. 2. Structure of simulated antenna: (a) 3D view of the antenna in free space and (b) front and lateral view of the antenna embedded in a metal cavity.

Moreover, by using the equation described in [9] it is possible to estimate the tag read range as

$$R_{read} = \frac{c}{2\omega} \cdot \sqrt{P_{tx,EIRP} \cdot D_{tag} \cdot \eta_{tag} \cdot \tau / P_{IC,sens}} \quad (2)$$

where c is the speed of light, $P_{tx,EIRP}$ is the equivalent isotropically radiated power of the reader device, D_{TAG} and η_{TAG} are the directivity and the radiation efficiency of the tag antenna, respectively, and $P_{IC,sens}$ is the reading sensitivity of the microchip, i.e. -18.5dBm [23]. As shown in Fig. 3b, the maximum reading range is close to 1.2m for each of the considered cavity sizes.

In Fig. 4, a similar analysis has been shown by varying the cavity depth, H_c , when the cavity size is 2mm wider than the tag size ($L_c=27\text{mm}$). Even though the resonance frequency basically remains stable within the ETSI UHF RFID band, the antenna gain significantly decreases when increasing the cavity depth (Fig. 4a). Such a variation affects the simulated read range which goes down to 0.6m when the tag is placed inside a 10mm-deep metal cavity (Fig. 4b).



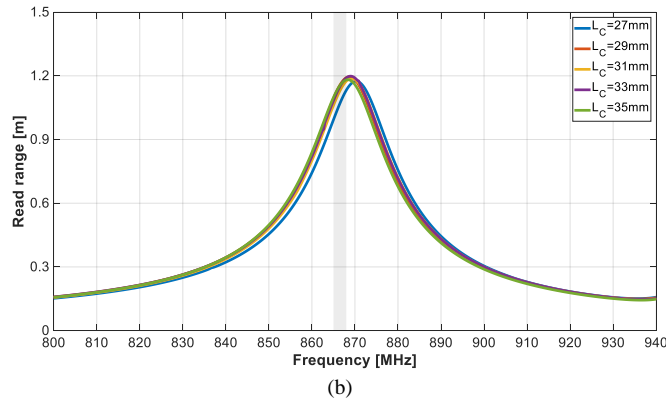


Fig. 3. Simulated antenna performance as a function of the square cavity edge, L_C , when the tag is completely embedded in the metal cavity ($H_C = 2\text{mm}$): (a) resonance frequency corresponding to the minimum PRC (solid black line), half-power bandwidth (red bars) and gain along the z -axis (dashed blue line); (b) read range estimated by using equation (2).

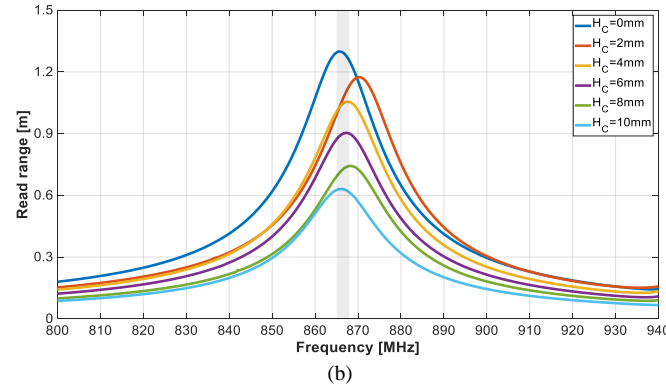
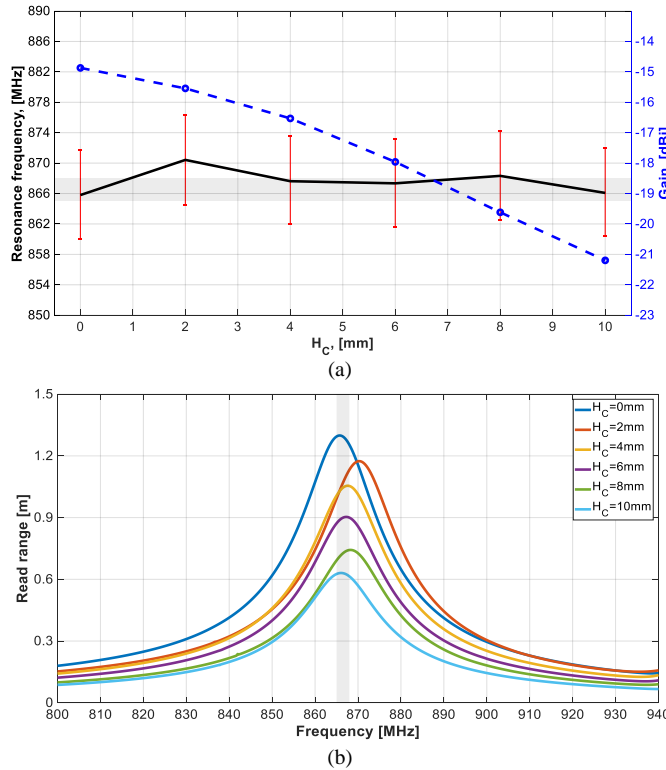


Fig. 4. Simulated antenna performance as a function of the square cavity depth, H_C : (a) resonance frequency corresponding to the minimum PRC (solid black line), half-power bandwidth (red bars) and gain along the z -axis (dashed blue line); (b) read range estimated by using equation (2). Note that $H_C = 0$ corresponds to the case of an on-metal tag.

As reported in [14], metal encased tags can be directly welded on the equipment or tools, which saves the effort for drilling holes on hard metals. Alternatively, tags can be covered by epoxy resin which allows for an easy attachment of the tag and preserves the tag from scraping operations that are usually adopted to smooth and polish the manufactured metal component. It is worth noting that the epoxy resin must be resistant to the high temperatures needed for the metal item shaping and refinement. From an electromagnetic point of view, the epoxy resin represents a superstrate layer, characterized by specific dielectric permittivity and loss tangent.

Thus, its presence must be taken into account during the design process of the tag antenna, to guarantee a satisfactory read range. Nevertheless, its presence is helpful to miniaturize the tag antenna size. To give evidence to the effect of the epoxy resin on the antenna performance, a superstrate with thickness H_R has been added on top of the UHF RFID tag, when the latter is placed on a $500 \times 500 \text{ mm}^2$ metal plate. Without loss of generality, a commercial epoxy resin has been considered [24], characterized by a relative dielectric permittivity $\epsilon_r = 4.8$ and loss tangent $\tan \delta = 0.015$. Such a resin features good heat resistance and long term high temperature structural strength retention even after prolonged exposure to moisture, aggressive chemicals and other severe environmental conditions. In Fig. 5, the gain variation and the miniaturization percentage are plotted as a function of the epoxy resin thickness, H_R . In Fig. 5b, the read range is computed by using equation (2). As expected, the presence of a resin layer introduces a frequency shift. The miniaturization percentage is shown in Fig. 5a as a function of the resin thickness. On the other hand, due to the losses introduced by the resin, the thicker is the superstrate layer the lower is the antenna gain.

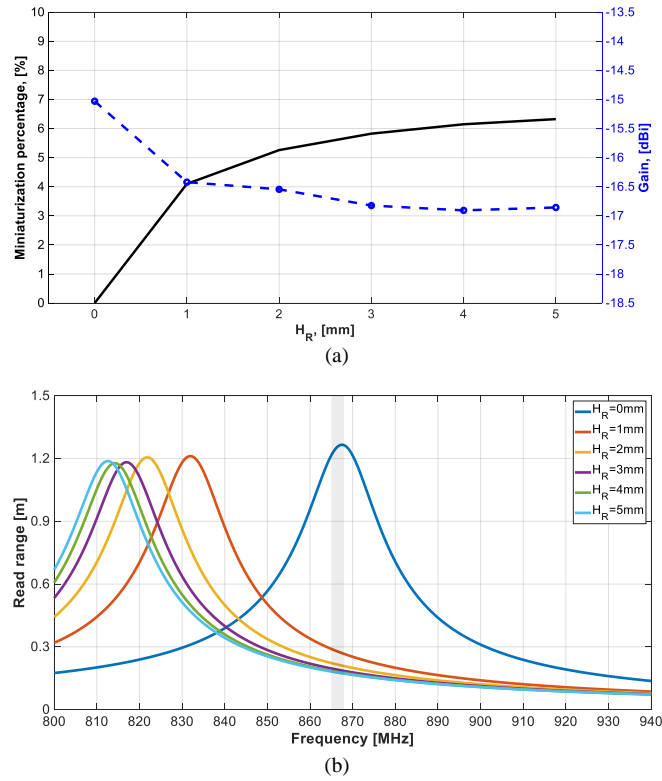


Fig. 5. Simulated antenna performance as a function of the epoxy resin thickness, H_R : (a) miniaturization factor (percentage miniaturization with respect to the absence of resin) and gain, and (b) read range as function of the frequency.

It is worth noting that from a practical point of view the resin thickness is related also to the cavity depth, since the resin is commonly used to completely fill the cavity and fix the tag to the metal object. To compensate for the miniaturization effect introduced by the presence of an epoxy resin layer above the tag antenna, the tag size can be uniformly scaled, as typically done in an antenna design process. However, a fine tuning of the antenna input impedance matching at UHF RFID ETSI band can be obtained by varying the lateral slits length (L_S), which have been initially introduced to reduce the physical size of the patch antenna. In Fig. 6 the read range as a function of the frequency is plotted for three values of the lateral slits length (L_S), where $L_S=11$ mm is the optimal value listed in TABLE I. It is worth noting that the shorter are the lateral slits (lower L_S), the higher is the tag resonant frequency and thus the maximum read range.

As a conclusion of this numerical analysis, it is apparent that a trade-off is needed among cavity size and depth, and epoxy resin thickness. It is worth noting that in some applications a long read range is not required, while a reliable tag detection in a well-defined area should be guaranteed [10], [25]. In particular, in the application scenario considered in this paper, a read range larger than 60cm can be enough to detect small/medium size manufactured metal components moving on a conveyor belt. Also, the metal cavity size and depth must be as small as possible, so that the tag can be applied even to relatively small components. The main parameters for the final antenna layout are listed in TABLE I.

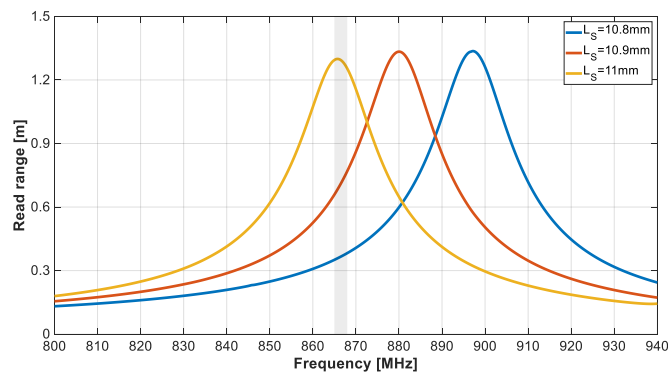


Fig. 6. Simulated antenna read range as a function of the frequency and of the lateral slits length, L_S .

TABLE I
ANTENNA MAIN PARAMETERS

Parameter	VALUE	PARAMETER	VALUE
L	23 mm	Δc	1 mm
H	1 mm	L_c	25 mm
L_M	500 mm	H_c	2.5 mm
H_M	12 mm	L_s	11 mm

The structure was optimized to be embedded in a $25 \times 25 \times 2.5$ mm³ cavity carved out of a metal plate ($150 \times 150 \times 7$ mm³) and filled with a commercial epoxy resin [24]. In Fig. 7a, the simulated input impedance is plotted as a function of the frequency. At the ETSI UHF RFID central frequency, the simulated input impedance is $Z_{in} \approx 10.3 + j189 \Omega$. In Fig. 7b-c, the simulated radiation patterns on the two principal planes are shown. Also, the estimated read range computed by using (2) is plotted in Fig. 8, as a function of the frequency, demonstrating that the 23×23 mm² tag optimized in a $25 \times 25 \times 2.5$ mm³ metal cavity and with a 1.5-mm thick epoxy resin superstrate can be read up to 1.5m at the UHF RFID ETSI band (*Config A*). However, the absence of the resin leads to a shift of the maximum read range toward higher frequencies, thus significantly deteriorating the performance at the UHF ETSI band (*Config B*). Specifically, the read range drops to less than 30cm when the epoxy resin is removed. A slightly better performance is obtained when the tag without epoxy resin is placed on metal (*Config C*), as highlighted in Fig 4, but it still may be not satisfactory for a practical application.

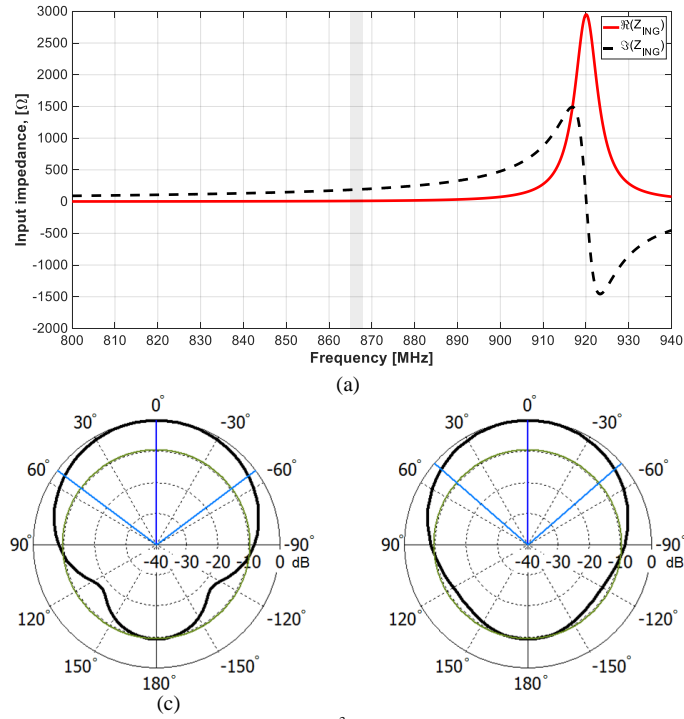


Fig. 7. Simulated performance when the tag is placed inside a $25 \times 25 \times 2.5$ mm³ cavity carved out of a metal plate ($150 \times 150 \times 7$ mm³) and covered by an epoxy resin ($\epsilon_r=4.8$, $\tan\delta=0.015$): (a) real and imaginary parts of the input impedance; radiation pattern at 866 MHz on (b) X-Z plane (E-plane) and (c) Y-Z plane (H-plane).

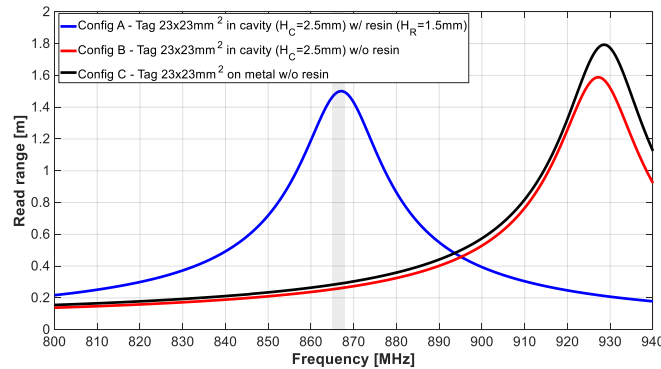


Fig. 8. Simulated read range as a function of the frequency for the $23 \times 23 \times 1$ mm³ tag in three configurations: the tag placed inside a $25 \times 25 \times 2.5$ mm³ cavity carved out of a metal plate ($150 \times 150 \times 7$ mm³) and covered by an epoxy resin ($\epsilon_r=4.8$, $\tan\delta=0.015$) (Config A); same configuration as Config A but without resin (Config B); same configuration as Config A but on metal and without resin.

III. EXPERIMENTAL ANALYSIS

The antenna described in Section II has been fabricated, and a picture is shown in Fig. 9. A $25 \times 25 \times 2.5$ mm³ cavity has been carved out of a $150 \times 150 \times 7$ mm³ metal component. The tag has been placed at the center of a cavity, keeping a distance of about 1 mm from the edges. Hence, the tag has been covered by a transparent epoxy resin (Fig. 9b). Measurements were performed using a commercial circularly polarized antenna connected to the Inpinj Speedway R420 reader [26] with a $P_{tx, EIRP} = 3.28$ W (2W ERP). The measured read range when the tag is placed inside the cavity and covered by the epoxy resin is about 1m. It is lower than the estimated one mainly due to uncertainty in the epoxy resin characteristics (*i.e.* thickness, dielectric permittivity and loss tangent) as well as in the actual dielectric characteristics of the ceramic substrate, which may differ from the nominal value. Anyway, the proposed in-metal UHF RFID tag is a good candidate for the considered applications, as measurement results demonstrated that it can guarantee a reading range larger than 60cm. Also, when the epoxy resin is removed, the read range drops to less than 40cm, demonstrating the importance of considering the resin since the first steps of the design process.

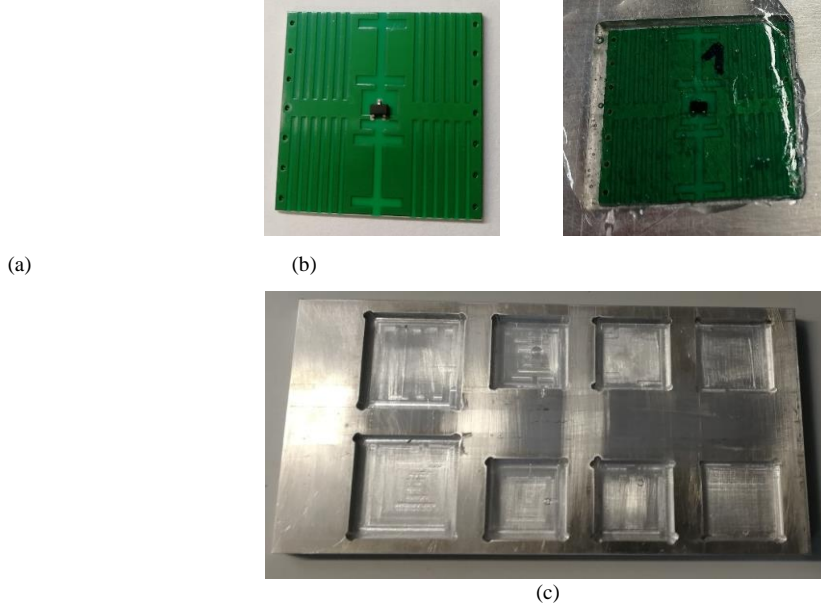


Fig. 9. Picture of the fabricated prototype when it is placed (a) on metal, without epoxy resin, and (b) inside a $25 \times 25 \times 2.5$ mm³ cavity carved out of a (c) $150 \times 150 \times 7$ mm³ metal plate, and covered by epoxy resin.

The analysis in Section II demonstrated that the tag performance is mainly affected by the cavity depth (H_c). For this reason, several cavities with different depths have been carved out from the metal object, and the read range has been measured when the tag is placed inside each of them. To account for the epoxy resin effect, a 1-mm layer of resin has been poured on the tag and left to dry for few hours.

The measured read range as a function of the cavity depth is plotted in Fig. 10 and compared with the simulated read range obtained from (2). When the tag is placed on metal ($H_c = 0$), the measured read range is close to 98cm while the simulated read range is of 130cm. As already discussed, this difference is mainly due to uncertainty in the epoxy resin and ceramic substrate characteristics. Anyway, the read range decreases when the cavity depth increases. When $H_c = 6$ mm, the measured and simulated read ranges reduce to 64cm and 90cm, respectively, which both approximately correspond to a 65% reduction.

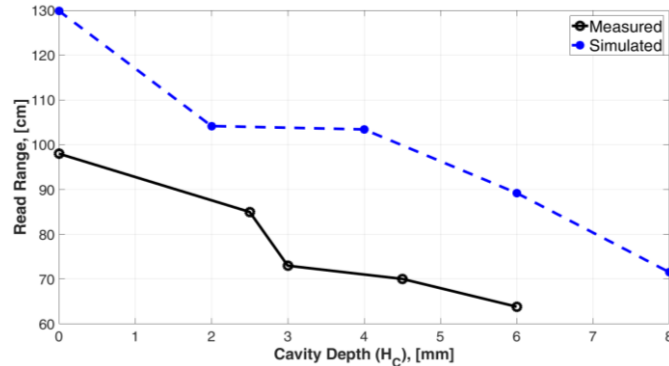


Fig. 10. Simulated and measured read ranges as a function of the 25×25 mm² cavity depth (H_c), when the $23 \times 23 \times 1$ mm³ tag shown in Fig. 9 is covered by a 1-mm thick epoxy resin layer.

IV. CONCLUSION

A $23 \times 23 \times 1$ mm³ ETSI UHF RFID in-metal tag has been designed for remote identification and tracking of manufactured metal components. The radiating element consists of two rectangular quarter-mode patch antennas properly arranged to limit the tag performance degradation when embedded in small metal cavities. A numerical analysis has been here described to investigate the effect of the cavity geometrical parameters on the tag power reflection coefficient, gain and estimated read range, demonstrating that the tag performance is mainly affected by

the cavity depth, which leads to a gain reduction. Moreover, the effect of the presence of a thin layer of epoxy resin used to fix the tag on the metal item has been investigated, giving evidence that its thickness and dielectric characteristics must be taken into account in the tag antenna design process. Experimental tests demonstrate that the tag can be detected at distances larger than 60cm if the cavity depth is smaller than 6mm.

REFERENCES

- [1] K. Finkenzeller, *RFID Handbook: Fundamentals and Applications in Contactless Smart Cards and Identification*, 2nd ed. Hoboken, NJ: Wiley, 2003
- [2] S. L. Chen, "A Miniature RFID Tag Antenna Design for Metal Objects Application," *IEEE Antennas and Wireless Propagation Letters*, vol. 8, pp. 1043-1045, 2009.
- [3] S. L. Chen, K. H. Lin and R. Mittra, "A low profile RFID tag designed for metal objects," *Asia Pacific Microwave Conference*, Singapore, 2009, pp. 226-228.
- [4] P. H. Yang, Y. Li, L. Jiang, W. C. Chew and T. T. Ye, "Compact Metal RFID Tag Antennas With a Loop-Fed Method," *IEEE Trans. on Antennas and Propagation*, vol. 59, no. 12, pp. 4454-4462, Dec. 2011.
- [5] C. W. Moh, E. H. Lim, F. L. Bong and B. K. Chung, "Miniature Coplanar-Fed Folded Patch for Metal Mountable UHF RFID Tag," *IEEE Trans. on Antennas and Propagation*, vol. 66, no. 5, pp. 2245-2253, May 2018.
- [6] F. L. Bong, E. H. Lim and F. L. Lo, "Flexible Folded-Patch Antenna With Serrated Edges for Metal-Mountable UHF RFID Tag," *IEEE Trans. on Antennas and Propagation*, vol. 65, no. 2, pp. 873-877, Feb. 2017.
- [7] A. A. Babar, T. Bjorninen, V. A. Bhagavati, L. Sydanheimo, P. Kallio and L. Ukkonen, "Small and Flexible Metal Mountable Passive UHF RFID Tag on High-Dielectric Polymer-Ceramic Composite Substrate," *IEEE Antennas and Wireless Propagation Letters*, vol. 11, pp. 1319-1322, 2012.
- [8] R. A. Ramirez, E. A. Rojas-Nastrucci and T. M. Weller, "UHF RFID Tags for On-/Off-Metal Applications Fabricated Using Additive Manufacturing," *IEEE Antennas and Wireless Propagation Letters*, vol. 16, pp. 1635-1638, 2017.
- [9] K. Jaakkola, "Small On-Metal UHF RFID Transponder With Long Read Range," *IEEE Trans. on Antennas and Propagation*, vol. 64, no. 11, pp. 4859-4867, Nov. 2016.
- [10] K. Jaakkola and P. Koivu, "Low-Cost and Low-Profile Near Field UHF RFID Transponder for Tagging Batteries and Other Metal Objects," *IEEE Trans. on Antennas and Propagation*, vol. 63, no. 2, pp. 692-702, Feb. 2015.
- [11] E. S. Yang and H. W. Son, "Dual-polarised metal-mountable UHF RFID tag antenna for polarisation diversity," *Electronics Letters*, vol. 52, no. 7, pp. 496-498, 4 1 2016.
- [12] F. L. Bong, E. H. Lim and F. L. Lo, "Compact Orientation Insensitive Dipolar Patch for Metal-Mountable UHF RFID Tag Design," *IEEE Trans. on Antennas and Propagation*, vol. 66, no. 4, pp. 1788-1795, April 2018
- [13] D. Kim and J. Yeo, "A Passive RFID Tag Antenna Installed in a Recessed Cavity in a Metal Platform," *IEEE Trans. on Antennas and Propagation*, vol. 58, no. 12, pp. 3814-3820, Dec. 2010.
- [14] H. Sun, B. Tao and O. M. Ramahi, "Proximity Coupled Cavity Backed Patch Antenna for Long Range UHF RFID Tag," *IEEE Trans. on Antennas and Propagation*, vol. 64, no. 12, pp. 5446-5449, Dec. 2016.
- [15] S. H. Jeong and H. W. Son, "UHF RFID Tag Antenna for Embedded Use in a Concrete Floor," *IEEE Antennas and Wireless Propagation Letters*, vol. 10, pp. 1158-1161, 2011.
- [16] J. S. Kim, W. Choi and G. Y. Choi, "UHF RFID tag antenna using two PIFAs embedded in metal objects," *Electronics Letters*, vol. 44, no. 20, pp. 1181-1182, September 25 2008.
- [17] J. S. Kim, W. Choi and G. Y. Choi, "Ceramic patch antenna for UHF RFID tag embedded in metal objects," *IEEE Antennas and Propagation Society International Symposium*, Charleston, SC, 2009, pp. 1-4.
- [18] V. Franchina, A. Michel, P. Nepa, and A. Salvatore, "Compact In-metal UHF RFID Tag for Manufactured Metal Components", presented at *2018 International Multidisciplinary Conference on Computer and Energy Science (SpliTech)*, Spalato, 2018
- [19] Best Technology, PCB vendor, <http://www.bestpcbs.com/index.htm>
- [20] K. V. S. Rao, P. V. Nikitin and S. F. Lam, "Antenna design for UHF RFID tags: a review and a practical application," *IEEE Trans. on Antennas and Propagation*, vol. 53, no. 12, pp. 3870-3876, Dec. 2005.
- [21] G. A. Casula, G. Montisci and G. Mazzarella, "A Wideband PET Inkjet-Printed Antenna for UHF RFID," *IEEE Antennas and Wireless Propagation Letters*, vol. 12, pp. 1400-1403, 2013.
- [22] K. H. Lin, S. L. Chen and R. Mittra, "A Capacitively Coupling Multifeed Slot Antenna for Metal RFID Tag Design," *IEEE Antennas and Wireless Propagation Letters*, vol. 9, pp. 447-450, 2010.
- [23] Alien Technology, Higgs[®]4 chip datasheet <http://www.alientechnology.com/products/ic/higgs-4/>
- [24] <http://www.lookpolymers.com/pdf/Master-Bond-EP46HT-Epoxy-Adhesive-for-Structural-Bonding.pdf>
- [25] A. Michel, P. Nepa, X. Qing and Z. N. Chen, "Considering High-Performance Near-Field Reader Antennas: Comparisons of Proposed Antenna Layouts for Ultrahigh-Frequency Near-Field Radio-Frequency Identification," *IEEE Antennas and Propagation Magazine*, vol. 60, no. 1, pp. 14-26, Feb. 2018.
- [26] RFID Reader, <https://www.impinj.com/platform/connectivity/speedway-r420/>